Published in final edited form as:
Org Biomol Chem. 2010 January 21; 8(2): 363–370. doi:10.1039/b918311f.

Electronically Tuned 1,3,5-Triarylpyrazolines as Cu(I)-Selective Fluorescent Probes†

Manjusha Verma, **Aneese F. Chaudhry**, **M. Thomas Morgan**, and **Christoph J. Fahrni**
School of Chemistry and Biochemistry, Petit Institute for Bioengineering and Bioscience, Georgia Institute of Technology, 901 Atlantic Drive, Atlanta, Georgia 30332, U.S.A

Christoph J. Fahrni: fahrni@chemistry.gatech.edu

Abstract

We have prepared and characterized a Cu(I)-responsive fluorescent probe, constructed using a large tetradentate, 16-membered thiazacrown ligand ([16]aneNS$_3$) and 1,3,5-triaryl-substituted pyrazoline fluorophores. The fluorescence contrast ratio upon analyte binding, which is mainly governed by changes of the photoinduced electron transfer (PET) driving force between the ligand and fluorophore, was systematically optimized by increasing the electron withdrawing character of the 1-aryl-ring, yielding a maximum 50-fold fluorescence enhancement upon saturation with Cu(I) in methanol and a greater than 300-fold enhancement upon protonation with trifluoroacetic acid. The observed fluorescence increase was selective towards Cu(I) over a broad range of mono- and divalent transition metal cations. Previously established Hammett LFERs proved to be a valuable tool to predict two of the PET key parameters, the acceptor potential $E(A/A^-)$ and the excited state energy ΔE_{00}, and thus to identify a set of pyrazolines that would best match the thermodynamic requirements imposed by the donor potential $E(D^+/D)$ of the thiazacrown receptor. The described approach should be applicable for rationally designing high-contrast pyrazoline-based PET probes selective towards other metal cations.

Introduction

Synthetic fluorescent probes are powerful analytical tools to detect metal cations with high selectivity and exquisite sensitivity down to the single molecule level.[1] Over the past decade, a broad range of fluorescent probes have been developed that exhibit high selectivity towards many of the nonredox-active metal cations, such as Ca(II),[2,3] Mg(II),[3,4] Zn(II),[5] or Cd(II).[6] In comparison, the fluorescence detection of redox-labile cations such as Cu(II/I)[7,8] or Fe(III/II)[9,10] remains challenging due to interference of metal-mediated quenching pathways, for example through electron transfer reactions, increased triplet conversion rates, or energy transfer processes involving energetically low-lying metal-centered states. These undesired quenching pathways can be reduced or even eliminated by using a rigid probe architecture that electronically decouples the metal binding site from the fluorophore.[11] Despite this spatial separation, metal binding to the receptor moiety can be effectively communicated through a photoinduced electron transfer (PET) switching mechanism. In this type of fluorescence switch, emission is quenched in absence of the analyte through PET from the metal receptor, which is acting as an electron donor, to the excited fluorophore, acting as the acceptor. Metal binding reduces the donating ability of the receptor, which in turn renders PET less favorable, resulting in reduced quenching and thus enhanced emission. For maximum sensitivity, the unbound probe should exhibit little or no background fluorescence and undergo a bright emission enhancement upon analyte binding.

Correspondence to: Christoph J. Fahrni, fahrni@chemistry.gatech.edu.

The fluorescence contrast between bound and unbound probe directly depends on the change in PET driving force ($-\Delta G_{et}$), the major parameter for optimizing the contrast ratio and switching properties.[12] According to the Rehm-Weller formalism, the driving force for PET depends on the ground state donor and acceptor potentials, $E(D^+/D)$ and $E(A/A^-)$, respectively, and the excited state energy ΔE_{00}, which corresponds to the transition energy between the vibrationally relaxed ground and excited states (eqn 1).[13]

$$\Delta G_{et} = E(D^+/D) - E(A/A^-) - \Delta E_{00} + w_p \quad (1)$$

The parameter w_p captures the Coulombic stabilization energy of the radical ion pair intermediate formed upon electron transfer. Based on equation (1), it can be readily seen that the increase in donor potential $E(D^+/D)$ upon metal binding results in a decrease of the PET driving force, $-\Delta G_{et}$, and thus a reduced ET quenching rate. By properly adjusting the remaining parameters, $E(A/A^-)$ and ΔE_{00}, the PET switching properties can in principle be optimized for any metal receptor; however, it is typically difficult to predict how structural changes of the fluorophore, such as attaching electron donating or withdrawing groups, will affect the two parameters.

To address this difficulty, we recently devised a systematic approach for optimizing the fluorescence contrast ratio through electronic tuning of the PET driving force.[14] Our strategy takes advantage of the rather unique electronic structure of 1,3,5-triarylpyrazoline fluorophores, which allow for adjustment of ΔE_{00} without significantly altering $E(A/A^-)$.[15,16] As illustrated with Chart 1 (left), this fluorophore platform is composed of a conjugated π-system with two aryl-substituents in the 1- and 3-positions, which are connected through the central pyrazoline core. The third aryl ring, which is attached in the 5-position, is electronically decoupled from the π-system through an sp^3-hybridized carbon atom and can be functionalized as a metal receptor to construct a PET fluorescent probe.[8,9,17] Most importantly, the HOMO and LUMO densities occupy two distinctly different regions of the π-system, where the HOMO is primarily localized on the 1-aryl and the LUMO on the 3-aryl ring. Due to this spatial separation, electron withdrawing substituents attached to the 1-aryl ring lead to an increase in ΔE_{00} but affect $E(A/A^-)$ only to a minor degree, whereas electron withdrawing substituents on the 3-aryl ring increase $E(A/A^-)$ without major changes to ΔE_{00}.[14–16] Hence, by choosing the appropriate substituents on the 3-aryl ring, such that $E(A/A^-)$ matches the donor potential of the metal receptor, ΔE_{00} can be increased stepwise by increasing the electron withdrawing ability of the 1-aryl ring, for example through attaching an increasing number of fluoro-substituents until the optimal contrast ratio is achieved. Based on this approach we were able to systematically optimize the fluorescence contrast of a simple pH-responsive probe of type **I** functionalized with a dimethylamino group ($R^3 = NMe_2$), which upon protonation gave a fluorescence enhancement of greater than 400-fold.[14]

This initial success prompted us to apply the above strategy towards optimizing the contrast ratio of a Cu(I)-responsive PET probe, a significantly more challenging problem compared to the initial pH-responsive probe. Because Cu(I) is a soft Lewis acid, we anticipated that the change in donor potential would be much smaller compared to the pH probe, which yielded an electrochemically inactive anilinium cation upon protonation. For this reason, fine tuning of the PET driving force appears to be particularly important for optimizing the contrast ratio of a Cu(I)-responsive probe. To selectively bind Cu(I) over other mono- and divalent metal cations, we chose a 16-membered trithiazacyclohexadecane ([16]aneNS$_3$) macrocycle as the receptor moiety (Chart 1, right). According to statistical multivariate examination of a large number of half-wave potentials of Cu^{2+}/Cu^+ couples complexed to N, S, and O-donor

ligands, large thioether macrocycles greatly favor Cu(I) over Cu(II) coordination.[18] In addition, we took advantage of recently established linear free energy relationships (LFERs)[16] to predict the PET thermodynamics for a set of fluoro-substituted pyrazolines that would best match the donor-potential of the Cu(I)-receptor moiety.

Results and Discussion

Predicting the PET Thermodynamics based on Hammett LFERs

Hammett substituent constants[19] (σ) have been widely used to correlate the electron withdrawing and donating abilities of substituents with the chemical reactivity and molecular properties of organic molecules.[20] Given the lack of experimental Hammett constants for polysubstituted aromatics, we derived computational substituent constants (σ^c) as recently described by Galabov et al.,[21] and established LFERs for predicting the PET thermodynamics of polyfluoro-substituted pyrazoline fluorophores.[16] Based on a training set of a total of 20 pyrazolines of type **I** (R^3 = H) with varying numbers of fluoro-substituents attached to the 1- and 3-aryl rings, we established a set of LFERs (eqn 2a and 2b) that related the experimental $E(A/A^-)$ and ΔE_{00} values with the corresponding pair of computational Hammett constants σ_1^c and σ_2^c, which reflect the electron withdrawing abilities of the 3- and 1-aryl rings, respectively.[16]

$$E(\mathrm{A/A^-})/V = -2.822 + 0.431 \cdot \sigma_1^c + 0.112 \cdot \sigma_2^c \quad (2a)$$

$$\Delta E_{00}/eV = 3.066 - 0.073 \cdot \sigma_1^c + 0.336 \cdot \sigma_2^c \quad (2b)$$

Furthermore, the sum of the above linear equations yielded a single LFER (eqn 2c) for the combined parameters ($E(A/A^-)+\Delta E_{00}$) with a correlation coefficient of r = 0.986 (training set mean unsigned error MUE = 0.028 eV).

$$(E(\mathrm{A/A^-})+\Delta E_{00})/eV = 0.244 + 0.358 \cdot \sigma_1^c + 0.448 \cdot \sigma_2^c \quad (2c)$$

Because the donor potential $E(D^+/D)$ is set by the type of metal receptor employed, the combined $E(A/A^-)$ and ΔE_{00} parameters directly define the tunable range of the PET driving force according to equation (1). Assuming that the Hammett constants σ_1^c and σ_2^c of each ring are varied between 0 and 1.19, corresponding to an unsubstituted and perfluorinated aryl ring, respectively, ΔG_{et} can be adjusted over a range of 0.96 V according to equation (2c). Since the 1-aryl ring is introduced during the last step of the pyrazoline synthesis (*vide infra*), adjustment of the PET driving force is best accomplished by varying R^2 (σ_2^c) while leaving R^1 (σ_1^c) constant. Although in this case the tunable range is reduced to approximately 0.53 eV, such a window is still sufficiently large for optimizing the contrast ratio. As pointed out above, the 3-aryl group locks the acceptor potential within a narrow range, and therefore, its substitution pattern must be carefully chosen to match the donor potential of the metal receptor. With an estimated donor potential of 0.45 V (vs. $Fc^{+/0}$) for the macrocyclic dialkylaniline receptor, a minimum PET driving force of $-\Delta G_{et}$ = 0 eV would require a 3-aryl ring Hammett constant of σ_1^c = 0.58 according to the LFER of eqn 2c. A comparison with the previously derived computational Hammett constants[16] for poly-fluoro-substituted aryl-rings suggests that a 2,5-difluoro substituted ring (σ_1^c = 0.58) would match best this value. Since it is not necessary to start the probe optimization at a zero driving force (which would not produce significant PET quenching), we decided to utilize a

slightly more electron withdrawing 3,5-difluoro substituted ring ($\sigma_1^c = 0.65$), thus yielding an estimated tunable potential window of $-\Delta G_{et}$ between 0.03 and 0.56 eV.

Synthesis

Based on the above considerations, we synthesized a series of pyrazolines derivatives **1a-f**, in which the [16]aneNS$_3$ macrocycle was combined with a 3,5-difluorophenyl substituent in the 3-position and a 1-aryl ring bearing increasing numbers of fluoro substituents (Scheme 1). The key step in accessing the racemic pyrazolines **1a-f** was the aldol condensation of benzaldehyde derivative **5** with 3,5-difluoroacetophenone followed by cyclization with the respective aryl hydrazines to give the desired pyrazolines. Aldehyde **5** was accessed directly through Vilsmeyer formylation of ligand **4**, which was obtained by macrocyclization of N,N-bis(3-iodopropyl)aniline[22] **3** with bis(3-mercaptopropyl)sulfide[23] **2**. Although the use of Cs_2CO_3 has been reported to be most effective for macrocyclizations to produce thiocrown ethers,[24] we observed comparable yields using the inexpensive base 1,1,3,3-tetramethylguanidine in refluxing acetonitrile, which provides the benefits of a less time consuming workup when the reaction is conducted on a multigram scale. Although we prepared the entire set of derivatives prior to their photophysical characterization, the 1-aryl ring critical for tuning the contrast ratio is introduced in the very last step of the synthetic protocol, thus facilitating the stepwise optimization of the photophysical properties.

Photophysical Characterization

The LFERs described by equations (2a-c) were derived from photophysical data acquired in acetonitrile; however, this solvent exhibits a significant affinity towards Cu(I) and can act as an effective competing ligand against the macrocycle. For this reason, we carried out the following photophysical studies in methanol as a substitute. The dielectric constants of the two solvents are almost identical, and thus the half-wave potentials and excited state energies of the derivatives are expected to remain similar within the accuracy of the LFER. A compilation of the acquired photophysical data is given in Table 1. As expected, the absorption and emission maxima shifted to higher energies with increasing number of fluoro-substituents on the 1-aryl-ring, and consequently, the zero-zero transition energies ΔE_{00} were also increased stepwise (Figure 1). The observed trend is consistent with a gradually decreasing charge delocalization from the 1-N-pyrazoline nitrogen to the 3-aryl ring for both the excited and ground state of the pyrazoline π-system.[14,16] Interestingly, the perfluoro-substituted derivative **1f** exhibits only a small increase in ΔE_{00} compared with compound **1e** containing only four fluoro-substituents. While the additional fluoro-substituent in the para position is expected to act as a sigma acceptor, the overall electron withdrawing ability of the aryl ring is attenuated through substantial π-donation, an effect we previously observed in a structurally related series of fluoro-substituted pyrazolines.[16]

In agreement with a stepwise increase of the PET driving force (*vide infra*), the quantum yields in neutral methanol gradually decreased as the number of fluoro-substituents increased from **1a** through **1d** (Table 1). For derivatives **1e** and **1f** the emission intensities and the associated signal/noise ratios were too low for accurate quantum yield determinations. Under acidic conditions, all compounds responded with a strong fluorescence enhancement, an observation that is consistent with protonation of the aniline donor, which in turn renders PET less favorable. The absorption and emission energies remained unchanged regardless of the proton concentration, indicating that none of the fluorophore heteroatoms are directly involved in a protonation equilibrium.

The fluorescence enhancement factor f_e, defined as the ratio of the quantum yield under acidic and neutral conditions, gradually increased up to 335 and closely followed the expected trend delineated in the earlier model study.[14] Although it was not possible to

obtain accurate enhancement factors for the strongly quenched derivatives **1e** and **1f**, inspection of the quantum yields under acidic conditions revealed substantially lower recovery yields, and thus presumably a reduced enhancement factor as expected based on the previously devised model.[14] For comparison, an analogous derivative of **1e** carrying the same fluoro substitution pattern but lacking the dialkylamino moiety showed a quantum yield of 69%,[16] thus indicating that the weak fluorescence emission of **1e** is due to PET quenching rather than an indirect effect of the increased number of fluoro substituents.

Fluorescence Response and Selectivity towards Metal Cations

Upon addition of excess $[Cu(I)(CH_3CN)_4]PF_6$, all probes exhibited a substantial increase in fluorescence; however, the enhancement factors were consistently lower compared to acidic conditions (Table 1). The degree of fluorescence enhancement again paralleled the number of fluoro-substituents, reaching a maximum f_e of 50 for the trifluoro-substituted derivative **1d**. The presence of additional fluoro-substituents (compounds **1e** and **1f**) resulted again in poor recovery of the fluorescence emission upon Cu(I) binding.

A titration of **1d** with $[Cu(I)(CH_3CN)_4]PF_6$ in methanol revealed a linear increase of the fluorescence intensity with increasing Cu(I) concentration (Figure 2). Consistent with a 1:1 binding stoichiometry, the saturation occurred at an equimolar ratio of Cu(I) and **1d**. As already observed for the protonation induced emission increase, the emission wavelength remained unchanged throughout the titration, suggesting no significant interactions between Cu(I) and the nitrogen atoms on the pyrazoline ring.

In addition, we tested the fluorescence response of **1d** towards a range of mono- and divalent metal cations. As illustrated by the bar graph in Figure 3, fluorophore **1d** responded with good selectivity towards Cu(I); only coordination of Fe(II) and Cu(II) led to a small emission increase. Competition experiments with equimolar amounts of Cu(I) and each of the respective metal cations showed in each case full recovery of the fluorescence emission, suggesting that the large thiazacrown preferentially binds to Cu(I) and effectively discriminates over all other metal cations tested.

Photoinduced Electron Transfer Thermodynamics

To determine the driving force of PET quenching in the absence of analyte according to equation (1), we measured the ground state donor and acceptor potentials of each derivative **1a–f** under neutral conditions (Table 2). Because the reduction potentials of the studied pyrazolines resided outside the potential window accessible in methanol, we used acetonitrile as the solvent. The estimated ΔG_{et} values closely mirror the above trend of the quantum yields under neutral conditions (Table 1). The smallest PET driving force yielded the highest quantum yield and vice versa. Consistent with previous results,[14] the PET driving force steadily increased with increasing number of fluoro-substituents attached to the 1-aryl ring. A closer inspection of the potential values revealed that the uniform increase in $-\Delta G_{et}$ was primarily due to changes in the excited state energy. Consistent with an electron transfer reaction originating from the aniline moiety for all of the derivatives, the measured donor potentials showed a narrow distribution with an average $E(D^+/D)$ of 0.48±0.01 V. The acceptor potentials also remained narrowly focused with an average $E(A/A^-)$ of −2.44±0.06 V.

To gauge the reliability of the Hammett LFER approach for predicting the PET parameters, we used the corresponding computational Hammett constants σ_1^c and σ_2^c of each derivative to calculate $E(A/A^-)$ and ΔE_{00} according to eqn 2a and 2b (Table 3). A comparison of the predicted acceptor potentials $E(A/A^-)$ with the experimental values listed in Table 2 showed very good agreement with a mean unsigned error of MUE 0.024 V. The average error for the

zero-zero transition energies ΔE_{00} is somewhat higher with MUE = 0.072 eV, and a closer inspection revealed that the energies were uniformly overestimated. The combined parameters estimated according to eqn 2c yielded a slightly lower MUE of 0.056 eV.

Altogether, the accuracy for prediction of the PET parameters $E(A/A^-)$ and ΔE_{00} for compounds **1a-f** compares well with the reliability trends observed in the previous test set of compounds,[16] which also showed a good agreement for $E(A/A^-)$ (MUE = 0.026) and a consistent overestimation for ΔE_{00} (MUE = 0.061). Furthermore, compound **1a** which was initially chosen as the starting point for the contrast optimization procedure agreed within 0.05 eV with the combined experimental parameters ($E(A/A^-)+\Delta E_{00}$), thus demonstrating that the LFER not only captured the overall trend of the PET driving force changes but predicted individual data with sufficeint accuracy to aid in choosing a fluoro-substituent pattern that matched the thermodynamic requirements of the thiazacrown aniline electron donor.

Conclusions

With their rigid molecular architecture and rationally tunable photophysical properties, 1,3,5-triaryl pyrazolines are well suited to meet the challenges associated with the design of PET probes geared towards the detection of metal cations such as Cu(I) that typically induce fluorescence quenching or yield only small emission enhancements. By stepwise increasing the electron withdrawing character of the 1-aryl ring, we were able to gradually adjust the PET quenching efficiency for the unbound probe while at the same time optimizing the fluorescence enhancement up to 50-fold upon Cu(I) binding. The previously established Hammett LFERs proved to be a valuable tool to predict the PET parameters $E(A/A^-)$ and ΔE_{00}, and thus to identify a set of pyrazolines that would best match the thermodynamic requirements imposed by the donor potential $E(D^+/D)$ of the thiazacrown receptor. Despite the fact that the previous LFERs were calibrated in acetonitrile, the predicted PET parameters $E(A/A^-)$ and ΔE_{00} agreed well with the experimental data in methanol. While it would be difficult to predict which of the pyrazoline derivatives might offer the best fluorescence enhancement for a given receptor, the LFER approach is well suited to narrow down the choices to a small set of derivatives. It is noteworthy that the 335-fold fluorescence enhancement in acidic methanol greatly exceeds the maximum contrast achieved for Cu(I)-binding for the same derivative **1d**. At present, we can only speculate about the reasons responsible for this large difference. Being a monovalent soft Lewis acid, Cu(I) would be expected to induce a smaller change in donor potential compared to protonation. Furthermore, the unbalanced coordination environment of the NS_3 donor set might weaken the interaction between the aniline nitrogen and Cu(I). Finally, Cu(I) might potentially engage in competitive quenching pathways and thus limit the maximum achievable quantum yield. We are currently addressing these questions with detailed time-resolved spectroscopic studies.

Experimental

Absorption and Fluorescence Spectroscopy

UV-vis absorption spectra were acquired at 25°C with a Varian Cary Bio50 spectrometer with constant-temperature accessory. Emission spectra were recorded with a PTI fluorimeter. The fluorescence spectra were corrected for the spectral response of the detection system and for the spectral irradiance of the excitation source (via a calibrated photodiode). For all measurements the path length was 1 cm with a cell volume of 3.0 mL. Sample solutions were filtered through 0.45 μm Teflon membrane filters to remove interfering dust particles. Quantum yields were determined using quinine sulfate dihydrate in 1.0 N H_2SO_4 as a fluorescence standard ($\Phi_f = 0.54 \pm 0.05$).[25]

Molar ratio titration with Cu(I)—A solution of **1d** (6.5 μM) in methanol was titrated with 0.1 molar equivalent aliquots of $[Cu(I)(CH_3CN)_4]PF_6$ (0.51 mM stock solution in 10% MeCN/MeOH (v/v)). After addition of each aliquot, the solution was allowed to equilibrate and an emission spectrum was acquired (excitation at 345 nm).

Metal ion selectivity studies—A solution of **1d** (6.5 μM) in methanol was equilibrated with an equimolar amount of the respective metal cation and the emission spectrum acquired (excitation at 345 nm). An equimolar amount of $[Cu(I)(CH_3CN)_4]PF_6$ (5.10 mM stock solution in MeCN) was subsequently added and the emission spectra acquired (excitation at 345 nm). Stock solutions of the following metal salts in water were used: $NaClO_4.H_2O$, $Mg(NO_3)_2.6H_2O$, $Ca(BF_4)_2.2H_2O$, $MnSO_4.2H_2O$, $Fe(BF_4)_2.6H_2O$, $Ni(NO_3)_2.6H_2O$, $Cu(TfO)_2$, $Zn(OTf)_2$, $CdCl_2$, and $HgCl_2$.

Cyclic Voltammetry

The donor and acceptor potentials of the pyrazoline fluorophores were determined through cyclic voltammetry in acetonitrile containing 0.1 M Bu_4NPF_6 as an electrolyte with a CH-instruments potentiostat (model 600A). The samples were measured under an inert gas at a concentration of 3 mM in a single compartment cell with a glassy carbon working electrode, a Pt counter electrode, and a $Ag/AgNO_3$ (10 mM in 0.1 M Bu_4NPF_6/CH_3CN) nonaqueous reference electrode. All potentials were referenced to the ferrocenium/ferrocene couple ($Fc^{+/0}$) as an internal or external standard.

Synthesis

Materials and Reagents—3,5-difluoroacetophenone, 3-fluorophenylhydrazine hydrochloride (Aldrich), 2,5-difluoro-phenylhydrazine, 2,3,5,6-tetrafluorophenylhydrazine, penta-fluorophenylhydrazine (Oakwood, West Columbia, SC); 2,3,5-trifluorophenylhydrazine was synthesized from 1,2,3,5-tetrafluorobenzene (Aldrich) following a published procedure.[26] NMR: δ in ppm vs $SiMe_4$ (0 ppm, 1H, 400 MHz). MS: selected peaks, m/z. Flash chromatography (FC): Merck silica gel (70–230 mesh). TLC: 0.25 mm, Merck silica gel 60 F254, visualizing at 254 nm or with 5% phosphomolybdic acid in EtOH.

Bis(3-mercaptopropyl)sulfide (2)[23]: A mixture of 3-chloro-1-propanol (25 mL, 300 mmol) and $Na_2S.9H_2O$ (35 g, 146 mmol) in 120 mL of aq. NaOH (0.5%) was heated at reflux for 12 h under nitrogen. The reaction mixture was cooled to 0°C, and aq. 37% HCl (100 mL) was added, followed by thiourea (34 g, 447 mmol). The mixture was refluxed under nitrogen for 2 days, cooled to 0°C, and NaOH pellets (93 g, 2.3 mol) were added with rapid stirring. The mixture was refluxed under nitrogen for 4 h and placed in a 2 L Erlenmeyer flask. After addition of crushed ice, the solution was acidified with 37% aq. HCl (100 mL). The product was extracted with tert-butyl methyl ether (3 × 120 mL). The extract was dried with Na_2SO_4 and concentrated under reduced pressure to yield the product as a colorless oil (21.3 g, 80%). ^1H NMR indicated the presence of a trace of 1,3-propanedithiol, and this was completely removed by heating the product to 150°C for 45 min under a stream of nitrogen (purified yield 18.0 g, 68%). R_f 0.41 (15:1 hexanes: EtOAc). IR ($CHCl_3$) ν_{max}/cm^{-1} 2929, 2845, 2549, 1435, 1344, 1295, 1251. ^1H NMR ($CDCl_3$, 400 MHz) δ 1.37 (t, J = 8.1Hz, 2H), 1.88 (p, J = 7.0Hz, 4H), 2.59–2.68 (m, 8H). ^{13}C NMR ($CDCl_3$, 100 MHz) δ 23.2, 30.0, 33.0. MS (70eV) 182 ([M^+], 100), 107 (65), 74 (67), 41 (65). EI HRMS m/z calcd for [M^+] $C_6H_{14}S_3$ 182.0258, found 182.0265.

N,N-Bis(3-iodopropyl)aniline (3)[22]: A mixture of N,N-bis(3-hydroxy-propyl)aniline[27] (8.10 g, 38.7 mmol) and Et_3N (22 mL, 4 equiv.) in CH_2Cl_2 (140 mL) was cooled in an ice bath under a stream of nitrogen, and methanesulfonyl chloride (9.0 mL, 3 equiv.) was added

dropwise with rapid stirring over a period of 5 min. The reaction mixture was stirred for 1 h and quenched by adding crushed ice. A solution of NaH_2PO_4 (6.7 g in 40 mL H_2O) was added. The organic layer was separated, dried with Na_2SO_4, and concentrated under reduced pressure. The residue was taken up in acetone (50 mL) and a solution of NaI (17.5 g, 3 equiv.) in acetone (50 mL) was added. The mixture was stirred overnight, diluted with water (200 mL) and extracted with *tert*-butyl methyl ether. The extract was washed twice with water and brine, dried with Na_2SO_4, and concentrated under reduced pressure to give the product as a yellow-brown oil. Yield 15.4 g (93%). R_f 0.44 (15:1 hexanes: EtOAc). IR ($CHCl_3$) ν_{max}/cm^{-1} 2926, 1598, 1504, 1228, 1199, 908, 748. ^1H NMR ($CDCl_3$, 400 MHz) δ 2.08 (p, *J* = 6.8 Hz, 4H), 3.20 (t, *J* = 6.6 Hz, 4H), 3.42 (t, *J* = 7.0 Hz, 4H), 6.69–6.74 (m, 3H), 7.19–7.25 (m, 2H). ^{13}C NMR ($CDCl_3$, 100 MHz) δ 3.7, 30.7, 51.6, 112.7, 116.7, 129.3, 147.4. MS (70eV) 429 ([M^+], 26), 274 (100), 146 (28). EI HRMS *m/z* calcd for [M^+] 428.9450, found 428.9470.

13-Phenyl-1,5,9-trithia-13-azacyclohexadecane (4): Iodide **3** (8.99 g, 21.0 mmol), thiol **2** (3.82 g, 21.0 mmol), and 1,1,3,3-tetramethylguanidine (5.3 mL, 2.0 equiv.) were each dissolved in CH_3CN, placed in 10 mL all-plastic syringes, and diluted to 10 mL. The resulting solutions were simultaneously and continuously added via syringe pump over a period of 60 h to a refluxing solution of 1,1,3,3-tetramethylguanidine (0.66 mL, 0.25 equiv) in acetonitrile (750 mL) under nitrogen. The reaction mixture was cooled and concentrated under reduced pressure. The residue was stirred with toluene (150 mL) for 1h. The precipitated salt was filtered out, and the filtrate was chromatographed on silica gel (hexanes-*tert*-butyl methyl ether) to give the product as a colorless, viscous oil. Yield 2.40 g (32%). R_f 0.35 (8:1 hexanes-MTBE), 0.34 (10:1 Hexanes: EtOAc). IR ($CHCl_3$) ν_{max}/cm^{-1} 2916, 2851, 1598, 1504, 1365, 1261, 910, 748. ^1H NMR ($CDCl_3$, 400 MHz) δ 1.92 (p, *J* = 7.0 Hz, 4H), 1.95 (p, *J* = 7.1 Hz, 4H), 2.62 (t, *J* = 6.9 Hz, 4H), 2.68 (t, *J* = 6.9 Hz, 4H), 2.69 (t, *J* = 7.0 Hz, 4H), 3.46 (t, *J* = 7.2 Hz, 4H), 6.66–6.71 (m, 3H), 7.19–7.25 (m, 2H). ^{13}C NMR ($CDCl_3$, 100 MHz) δ 27.5, 29.6, 29.8, 30.8, 31.0, 50.4, 112.5, 116.2, 129.2, 148.1. MS (70eV) 355 ([M^+], 100), 221 (18), 193 (17), 180 (27), 146 (46), 120 (29), 106 (26), 77 (11). EI HRMS m/z calcd for [M^+] $C_{18}H_{29}NS_3$ 355.1462, found 355.1458.

4-(1,5,9-Trithia-13-azacyclohexadecan-13-yl)benzaldehyde (5): Dimethylformamide (8.5 mL, 110 mmol) was cooled in an ice bath, and $POCl_3$ (5.0 mL, 55 mmol) was added over a period of 30 min. The resulting mixture was added to a solution of **4** (2.40 g, 6.75 mmol) in DMF (8 mL). After stirring for 45 min at 75°C, the mixture was cooled to room temperature, poured into water (200 mL), and made basic with NaOH. CH_2Cl_2 (50 mL) was added, and the mixture was stirred for 1 h. The organic layer was separated, and the aqueous layer was extracted with CH_2Cl_2 (2 × 50 mL). The combined organic extracts were concentrated under reduced pressure, and the residue was taken up in benzene (25 mL) and washed with water. The solution was dried with Na_2SO_4 and concentrated under reduced pressure to give the product as a yellow-brown oil. Yield: 2.56 g (99%). R_f 0.44 (2:1 hexanes: EtOAc). IR ($CHCl_3$) ν_{max}/cm^{-1} 2935, 2848, 1667, 1597, 1524, 1406, 1364, 1198, 1168, 818. ^1H NMR ($CDCl_3$, 400 MHz) δ 1.93 (p, *J* = 6.9 Hz, 4H), 1.99 (p, *J* = 7.0 Hz, 4H), 2.64 (t, *J* = 6.6 Hz, 4H), 2.70 (t, *J* = 6.9 Hz, 4H), 2.72 (t, *J* = 7.0 Hz, 4H), 3.61 (t, *J* = 7.5 Hz, 4H), 6.68 (d, *J* = 9.0 Hz, 2H), 7.72 (d, *J* = 9.0 Hz, 2H), 9.73 (s, 1H). ^{13}C NMR ($CDCl_3$, 100 MHz) δ 26.9, 29.1, 29.4, 30.5, 30.9, 49.9, 110.8, 124.9, 132.0, 152.3, 189.8. MS (70eV) 383 ([M^+], 100), 249 (15), 208 (26), 174 (44), 134 (25), 87 (13), 41 (14). EI HRMS m/z calcd for [M^+] $C_{10}H_{29}NOS_3$ 383.1411, found 383.1392.

(*E*)-3-(4-(1,5,9-Trithia-13-azacyclohexadecan-13-yl)-phenyl)-1-(3,5-difluorophenyl)prop-2-en-1-one (6): Aldehyde **5** (385 mg, 1.0 mmol) and 3,5-difluoroacetophenone (172 mg, 1.1 mmol) were dissolved in 4 mL of ethanol-benzene (1:1) at 40°C. Pyrrolidine (0.2 mL, 2 equiv) was then added, the reaction flask was sealed, and the

mixture was stirred at 40°C for 24 hours. The mixture was diluted with 25 mL of ethanol and concentrated to a volume of 10 mL. An additional 15 mL of ethanol was added, and the mixture was stirred at 0°C for 4 hours. The orange crystalline product was filtered off and dried under vacuum. Yield: 384 mg (73%). IR (KBr) ν_{max}/cm^{-1} 2920, 1569, 1521, 1359, 1297, 1158, 984, 809. ^{1}H NMR ($CDCl_3$, 400 MHz) δ 1.93 (p, *J* = 6.9 Hz, 4H), 1.98 (p, *J* = 7.0 Hz, 4H), 2.64 (t, *J* = 6.6 Hz, 4H), 2.70 (t, *J* = 7.0 Hz, 4H), 2.72 (t, *J* = 7.1 Hz, 4H), 3.58 (t, *J* = 7.4 Hz, 4H), 6.66 (d, *J* = 8.9 Hz, 2H), 6.99 (tt, *J* = 8.5, 2.4 Hz, 1H), 7.50 (ddd, *J* = 7.9, 2.4, 1.2 Hz, 2H), 7.53 (d, *J* = 8.9 Hz, 2H), 7.80 (d, *J* = 15.4 Hz, 1H). ^{13}C NMR ($CDCl_3$, 100 MHz) δ 27.2, 29.4, 29.6, 30.8, 31.1, 50.1, 107.3 (t, J_{CF} = 25.5 Hz), 111.1 (dd, J_{CF} = 18.7, 7.1 Hz), 111.7, 115.3, 122.0, 131.0, 142.2 (t, J_{CF} = 7.4 Hz), 147.1, 150.3, 162.9 (dd, J_{CF} = 250.2, 12.0 Hz), 187.5 (t, J_{CF} = 1.9 Hz, broad). ^{19}F NMR ($CDCl_3$, 376 MHz) δ −109.2 (t, *J* = 7.4 Hz, 2F). MS (70 eV) 521 ([M^+], 100), 387 (23), 312 (30), 286 (35), 141 (21). EI HRMS *m/z* calcd for [M^+] $C_{27}H_{33}NOS_3$ 521.1692, found 521.1726.

Synthesis of racemic 1,3,5-triarylpyrazolines from 5 and polyfluorophenylhydrazines (General method): A mixture of the chalcone (0.09 mmol) and fluoro-substituted phenylhydrazine (1.3 molar eq.), hydrochloric acid (1.3 molar eq.) and K_2CO_3 (0.25 molar eq.) in anhydrous ethanol (1 mL) was heated at 90°C for 12 h (Note: if phenylhydrazine was used as HCl salt, no additional HCl was added). Upon completion of the reaction (TLC), the mixture was cooled to room temperature and diluted with water (10 mL). The precipitated product was filtered off, and washed consecutively with aq. HCl (1 M) and NaOH (5%). In cases where no precipitate was formed, the reaction mixture was extracted twice with EtOAc. The combined organic phases were washed with aq. HCl (1 M) and NaOH (5%), dried (Na_2SO_4), and concentrated under reduced pressure. The crude product was purified by flash chromatography.

(±)-13-(4-(3-(3,5-difluorophenyl)-1-phenyl-4,5-dihydro-1*H*-pyrazol-5-yl)phenyl)-1,5,9-trithia-13-azacyclohexa-decane (1a): Yield: 83%. IR ($CHCl_3$) ν_{max}/cm^{-1} 2917, 2849, 1615, 1595, 1516, 1393, 1199, 1118, 981, 910, 734. ^{1}H-NMR ($CDCl_3$, 400 MHz) δ 1.93–1.86 (m, 8H),), 2.57 (t, *J* = 6.8 Hz, 4H), 2.69–2.65 (m, 8H),), 3.03 (dd, *J* = 17.0, 7.0 Hz, 1H), 3.40 (t, *J* = 7.2 Hz, 4H), 3.69 (dd, *J* = 17.0, 12.4 Hz, 1H), 5.23 (dd, *J* = 12.3, 6.9 Hz, 1H), 6.58 (d, *J* = 14.7 Hz, 2H), 6.71 (tt, *J* = 8.8, 2.4 Hz, 1H),), 6.78 (tt, *J* = 7.2, 1.2 Hz, 1H), 7.08 (d, *J* = 6.6 Hz, 4H), 7.17 (t, *J* = 8.7 Hz, 4H). ^{19}F NMR ($CDCl_3$, 376 MHz) δ −110.4 (t, *J* = 7.7 Hz, 2F). MS (70 eV) 611 ([M^+], 100), 477 (19), 376 (12), 257 (15). EI HRMS *m/z* calcd for [M^+] $C_{33}H_{39}F_2N_3S_3$ 611.2274, found 611.2229.

(±)-13-(4-(3-(3,5-difluorophenyl)-1-(3-fluorophenyl)-4,5-dihydro-1*H*-pyrazol-5-yl)phenyl)-1,5,9-trithia-13-azacyclo-hexadecane (1b): Yield: 89%. IR ($CHCl_3$) ν_{max}/cm^{-1} 2927, 1611, 1563, 1520, 1393, 1261, 1180, 1117, 986, 910, 851, 732. ^{1}H NMR ($CDCl_3$, 400 MHz) δ 1.86–1.95 (m, 8H), 2.56 (t, *J* = 6.8 Hz, 4H), 2.67 (t, *J* = 6.9 Hz, 4H), 2.68 (t, *J* = 7 Hz, 4H), 3.07 (dd, *J* = 17.3, 6.6 Hz, 1H), 3.44 (t, *J* = 7.2 Hz, 4H), 3.73 (dd, *J* = 17.1, 12.3 Hz, 1H), 5.22 (dd, *J* = 12.3, 6.6 Hz, 1H), 6.48 (tdd, *J* = 8.4, 2.5, 0.8 Hz, 1H), 6.61 (d, *J* = 8.9 Hz, 2H), 6.76 (tt, *J* = 8.8, 2.3 Hz, 1H), 6.79 (ddd, *J* = 8.4, 2.2, 0.8 Hz, 1H), 6.86 (dt, *J* = 11.8, 2.3 Hz, 1H), 7.08 (d, *J* = 8.9 Hz, 2H), 7.10–7.13 (m, 1H), 7.17–7.23 (m, 2H). ^{19}F NMR ($CDCl_3$, 376 MHz) δ −110.1 (t, *J* = 7.8 Hz, 2F), −113.0 (ddd, *J* = 12.1, 8.4, 6.6 Hz, 1F). MS (70 eV) 629 ([M^+], 100), 495 (24), 418 (22), 392 (22), 275 (15). EI HRMS *m/z* calcd for [M^+] $C_{33}H_{38}F_3N_3S_3$ 629.2180, found 629.2146.

(±)-13-(4-(3-(3,5-difluorophenyl)-1-(2,5-difluorophenyl)-4,5-dihydro-1*H*-pyrazol-5-yl)phenyl)-1,5,9-trithia-13-aza-cyclohexadecane (1c): Yield: 63%. IR ($CHCl_3$) ν_{max}/cm^{-1} 2919, 2851, 1619, 1505, 1441, 1377, 1198, 1118, 989, 910, 733. ^{1}H NMR ($CDCl_3$, 400 MHz) δ 1.92–1.82 (m, 8H), 2.55 (t, *J* = 6.8 Hz, 4H), 2.65 (dt, *J* = 6.9, 1.8 Hz, 8H), 3.19 (dd, *J* = 16.9, 3.8 Hz, 1H), 3.37 (t, *J* = 7.1 Hz, 4H), 3.68 (dd, *J* = 16.8, 11.7 Hz, 1H), 5.62 (td, *J* =

11.6, 3.7 Hz, 1H), 6.48–6.42 (m, 3H), 6.84–6.75 (m, 2H), 6.95 (d, *J* = 8.7 Hz, 2H), 7.24–7.22 (m, 2H), 7.33 (ddd, *J* = 9.9, 6.5, 3.1 Hz, 1H). ^{19}F NMR ($CDCl_3$, 376 MHz) δ −109.9 (t, *J* = 8.0 Hz, 2F), −118.6 (m, 1F), −130.9 (m, 1F). MS (70 eV) 647 ([M^+], 100), 513 (28), 412 (20), 293 (12). EI HRMS *m/z* calcd for [M^+] $C_{33}H_{37}F_4N_3S_3$ 647.2086, found 647.2079.

(±)-13-(4-(3-(3,5-difluorophenyl)-1-(2,3,5-trifluoro-phenyl)-4,5-dihydro-1*H*-pyrazol-5-yl)phenyl)-1,5,9-trithia-13-azacyclohexadecane (1d): Yield: 59%. IR ($CHCl_3$) ν_{max}/cm^{-1} 2920, 2850, 1615, 1516, 1453, 1191, 1142, 990, 732. ^{1}H NMR ($CDCl_3$, 400 MHz) δ 1.90–182 (m, 8H), 2.56 (t, *J* = 6.8 Hz, 4H), 2.66–2.62 (m, 8H), 3.19 (dd, *J* = 17.0, 3.7 Hz, 1H), 3.39 (t, *J* = 7.1 Hz, 4H), 3.69 (dd, *J* = 16.9, 11.6 Hz, 1H), 5.62 (td, *J* = 11.6, 3.7 Hz, 1H), 6.37–6.30 (m, 1H), 6.49 (d, *J* = 14.8 Hz, 2H), 6.79 (tt, *J* = 8.7, 2.3 Hz, 1H), 6.95 (d, *J* = 11.5 Hz, 2H), 7.14–7.08 (m, 1H), 7.23–7.18 (m, 2H). ^{19}F NMR ($CDCl_3$, 376 MHz) δ −109.8 (t, *J* = 7.6 Hz, 2F), −116.0 (dddd, *J* = 11.7, 10.9, 8.2, 3.0 Hz, 1F), −135.2 (ddt, *J* = 20.0, 10.3, 3.0 Hz, 1F), −156.6 (dddd, *J* = 20.0, 11.7, 9.8, 5.2 Hz, 1F). MS (70 eV) 665 ([M^+], 100), 531 (30), 430 (22), 311 (14). EI HRMS *m/z* calcd for [M^+] $C_{33}H_{36}F_5N_3S_3$ 665.1992, found 665.1978.

(±)-13-(4-(3-(3,5-difluorophenyl)-1-(2,3,5,6-tetrafluoro-phenyl)-4,5-dihydro-1*H*-pyrazol-5-yl)phenyl)-1,5,9-trithia-13-azacyclohexadecane (1e): Yield: 66%. IR ($CHCl_3$) ν_{max}/cm^{-1} 2922, 2852, 1615, 1505, 1372, 1262, 1146, 1119, 990, 910, 733. ^{1}H NMR ($CDCl_3$, 400 MHz) δ 1.91–1.83 (m, 8H), 2.56 (t, *J* = 6.7 Hz, 4H), 2.67–2.63 (m, 8H), 3.19 (dd, *J* = 17.0, 7.2 Hz, 1H), 3.39 (t, *J* = 7.1 Hz, 4H), 3.62 (dd, *J* = 16.9, 11.8 Hz, 1H), 5.46 (dd, *J* = 11.9, 7.4 Hz, 2H), 6.50 (d, *J* = 8.7 Hz, 2H), 6.73–6.64 (m, 1H), 6.77 (tt, *J* = 10.9, 2.2 Hz, 1H), 7.06 (d, *J* = 8.6 Hz, 2H), 7.19–7.17 (m, 2H). ^{19}F NMR ($CDCl_3$, 376 MHz) δ −109.9 (t, *J* = 7.7 Hz, 2F), −140.6 (ddd, *J* = 21.2, 10.8, 8.8 Hz, 2F), −149.0 (ddd, *J* = 21.2, 8.8, 8.4 Hz, 2F). MS (70 eV) 683 ([M^+], 100), 549 (29), 448 (26). EI HRMS *m/z* calcd for [M^+] $C_{33}H_{35}F_6N_3S_3$ 683.1897, found 683.1843.

(±)-13-(4-(3-(3,5-difluorophenyl)-1-(perfluorophenyl)-4,5-dihydro-1*H*-pyrazol-5-yl)phenyl)-1,5,9-trithia-13-aza-cyclohexadecane (1f): Yield: 90%. IR ($CHCl_3$) ν_{max}/cm^{-1} 2919, 2852, 1615, 1516, 1372, 1262, 1187, 1119, 1064, 989, 733. ^{1}H NMR ($CDCl_3$, 400 MHz) δ 1.86–1.94 (m, 8H), 2.58 (t, *J* = 6.8 Hz, 4H), 2.65–2.69 (m, 8H), 3.21 (dd, *J* = 16.9, 8.2 Hz, 1H), 3.42 (t, *J* = 7.1 Hz, 4H), 3.62 (dd, *J* = 16.8, 3.6 Hz, 1H), 5.34 (dd, *J* = 11.5, 8.8 Hz, 1H), 6.52 (d, *J* = 8.8 Hz, 2H), 6.79 (tt, *J* = 8.7, 2.3 Hz, 1H), 7.09 (d, *J* = 8.7 Hz, 2H), 7.16–7.23 (m, 2H). ^{19}F NMR ($CDCl_3$, 376 MHz) δ −109.9 (t, *J* = 8.0 Hz, 2F), −148.2 (dd, *J* = 22.0, 4.9 Hz, 2F), −161.2 (t, *J* = 22.0 Hz, 1F), −163.7 (td, *J* = 22.0, 4.9 Hz, 2F). MS (70 eV) 701 ([M^+], 100), 567 (25), 466 (24). EI HRMS *m/z* calcd for [M^+] $C_{33}H_{34}F_7N_3S_3$ 701.1803, found 701.1789.

Supplementary Material

Refer to Web version on PubMed Central for supplementary material.

Acknowledgments

Financial support from the National Institutes of Health (R01GM067169) is gratefully acknowledged.

References

1. de Silva AP, Gunaratne HQN, Gunnlaugsson T, Huxley AJM, McCoy CP, Rademacher JT, Rice TE. Chem Rev. 1997; 97:1515. [PubMed: 11851458] Rurack K. Spectrochim Acta A. 2001; 57:2161.de Silva AP, Vance TP, West MES, Wright GD. Org Biomol Chem. 2008; 6:2468.

[PubMed: 18600265] Domaille DW, Que EL, Chang CJ. Nat Chem Biol. 2008; 4:168. [PubMed: 18277978]

2. Grynkiewicz G, Poenie M, Tsien RY. J Biol Chem. 1985; 260:3440. [PubMed: 3838314] Takahashi A, Camacho P, Lechleiter JD, Herman B. Physiol Rev. 1999; 79:1089. [PubMed: 10508230]
3. Kim HM, Kim BR, Hong JH, Park JS, Lee KJ, Cho BR. Angew Chem Int Ed Engl. 2007; 46:7445. [PubMed: 17680568]
4. Komatsu H, Iwasawa N, Citterio D, Suzuki Y, Kubota T, Tokuno K, Kitamura Y, Oka K, Suzuki K. J Am Chem Soc. 2004; 126:16353. [PubMed: 15600336] Farruggia G, Iotti S, Prodi L, Montalti M, Zaccheroni N, Savage PB, Trapani V, Sale P, Wolf FI. J Am Chem Soc. 2006; 128:344. [PubMed: 16390164] Liu Y, Han M, Zhang HY, Yang LX, Jiang W. Org Lett. 2008; 10:2873. [PubMed: 18540629]
5. Jiang PJ, Guo ZJ. Coord Chem Rev. 2004; 248:205.Lim NC, Freake HC, Bruckner C. Chem Eur J. 2004; 11:38.Kikuchi K, Komatsu K, Nagano T. Curr Opin Chem Biol. 2004; 8:182. [PubMed: 15062780] Nolan EM, Lippard SJ. Acc Chem Res. 2009; 42:193. [PubMed: 18989940]
6. Lu C, Xu Z, Cui J, Zhang R, Qian X. J Org Chem. 2007; 72:3554. [PubMed: 17381157] Taki M, Desaki M, Ojida A, Iyoshi S, Hirayama T, Hamachi I, Yamamoto Y. J Am Chem Soc. 2008; 130:12564. [PubMed: 18761452] Xue L, Liu Q, Jiang H. Org Lett. 2009; 11:3454. [PubMed: 19719190] Cheng T, Xu Y, Zhang S, Zhu W, Qian X, Duan L. J Am Chem Soc. 2008; 130:16160. [PubMed: 19006390]
7. Cody J, Fahrni CJ. Tetrahedron. 2004; 60:11099.Zeng L, Miller EW, Pralle A, Isacoff EY, Chang CJ. J Am Chem Soc. 2006; 128:10. [PubMed: 16390096] Martínez R, Zapata F, Caballero A, Espinosa A, Tarraga A, Molina P. Org Lett. 2006; 8:3235. [PubMed: 16836374] Yu M, Shi M, Chen Z, Li F, Li X, Gao Y, Xu J, Yang H, Zhou Z, Yi T, Huang C. Chem Eur J. 2008; 14:6892.Zhao Y, Zhang XB, Han ZX, Qiao L, Li CY, Jian LX, Shen GL, Yu RQ. Anal Chem. 2009; 81:7022. [PubMed: 19634898]
8. Yang L, McRae R, Henary MM, Patel R, Lai B, Vogt S, Fahrni CJ. Proc Natl Acad Sci USA. 2005; 102:11179. [PubMed: 16061820]
9. Bricks JL, Kovalchuk A, Trieflinger C, Nofz M, Büschel M, Tolmachev AI, Daub J, Rurack K. J Am Chem Soc. 2005; 127:13522. [PubMed: 16190715]
10. Zhang M, Gao Y, Li M, Yu M, Li F, Li L, Zhu M, Zhang J, Yi T, Huang C. Tetrahedron Lett. 2007; 48:3709.Jung HJ, Singh N, Jang DO. Tetrahedron Letters. 2008; 49:2960.Singh N, Kaur N, Callan JF. J Fluoresc. 2009; 19:649. [PubMed: 19139975]
11. Rurack K, Kollmannsberger M, Resch-Genger U, Daub J. J Am Chem Soc. 2000; 122:968.Rurack K, Resch-Genger U. Chem Soc Rev. 2002; 31:116. [PubMed: 12109205]
12. Kollmannsberger M, Rurack K, Resch-Genger U, Rettig W, Daub J. Chem Phys Lett. 2000; 329:363.Hirano T, Kikuchi K, Urano Y, Nagano T. J Am Chem Soc. 2002; 124:6555. [PubMed: 12047174] Kenmoku S, Urano Y, Kanda K, Kojima H, Kikuchi K, Nagano T. Tetrahedron. 2004; 60:11067.
13. Rehm D, Weller A. Isr J Chem. 1970; 8:259.
14. Cody J, Mandal S, Yang L, Fahrni CJ. J Am Chem Soc. 2008; 130:13023. [PubMed: 18767839]
15. Fahrni CJ, Yang LC, VanDerveer DG. J Am Chem Soc. 2003; 125:3799. [PubMed: 12656613]
16. Verma M, Chaudhry AF, Fahrni CJ. Org Biomol Chem. 2009; 7:1536. [PubMed: 19343239]
17. de Silva AP, de Silva SA, Dissanayake AS, Sandanayake K. Chem Commun. 1989:1054.de Silva AP, Gunaratne HQN. Chem Commun. 1990:186.de Silva AP, Gunaratne HQN, Maguire GEM. Chem Commun. 1994:1213.de Silva AP, Gunaratne HQN, Gunnlaugsson T, Nieuwenhuizen M. Chem Commun. 1996:1967.Rurack K, Bricks JL, Schulz B, Maus M, Reck G, Resch-Genger U. J Phys Chem A. 2000; 104:6171.
18. Addison AW. Inorg Chim Acta. 1989; 162:217.
19. Hammett LP. J Am Chem Soc. 1937; 59:96.
20. Craik DJ, Brownlee RTC. Prog Phys Org Chem. 1983; 14:1.Hansch C, Leo A, Taft RW. Chem Rev. 1991; 91:165.Gross KC, Seybold PG. Int J Quantum Chem. 2001; 85:569.Sullivan JJ, Jones AD, Tanji KK. J Chem Inf Comput Sci. 2000; 40:1113. [PubMed: 11045804] Fernández I, Frenking G. J Org Chem. 2006; 71:2251. [PubMed: 16526770]
21. Galabov B, Ilieva S, Schaefer HF. J Org Chem. 2006; 71:6382. [PubMed: 16901119]

22. Everett JL, Ross WCJ. J Chem Soc. 1949:1972.
23. Goodrow MH, Musker WK. Synthesis. 1981:457.
24. Buter J, Kellogg RM. J Org Chem. 1981; 46:4481.
25. Demas JN, Crosby GA. J Phys Chem. 1971; 75:991.
26. Burdon J, Hollyhead WB. J Chem Soc. 1965:6326.
27. Jones GB, Chapman BJ, Mathews JE. J Org Chem. 1998; 63:2928.

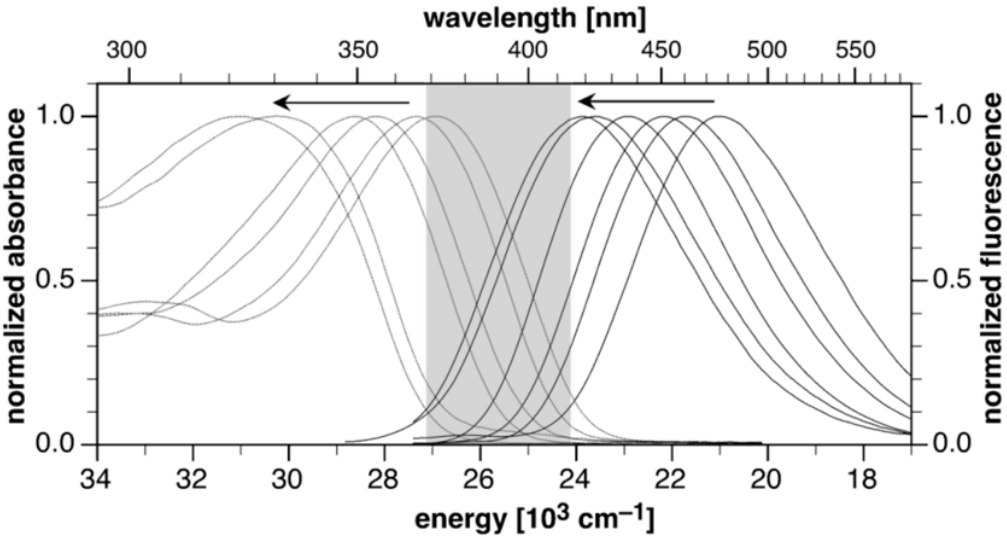

Fig. 1.

Normalized absorption (dotted traces) and emission spectra (solid traces) of compounds **1a–f**. The arrows indicate the direction of the band shift with increasing number of fluoro substituents. The shaded area indicates the tunable range of the excited-state energy ΔE_{00}.

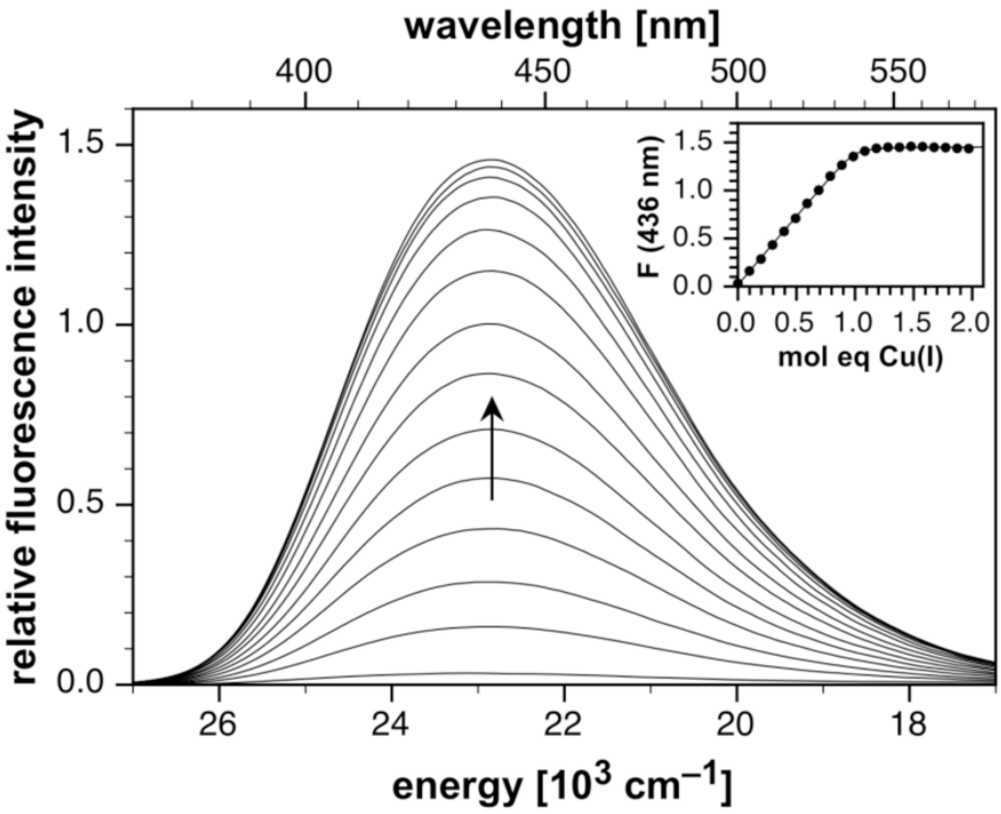

Fig. 2.

Fluorescence titration of pyrazoline **1d** (6.5 μM) with $[Cu(I)(CH_3CN)_4]PF_6$ in MeOH (298 K, excitation at 345 nm). Inset: Molar-ratio plot for the fluorescence intensity change at 436 nm.

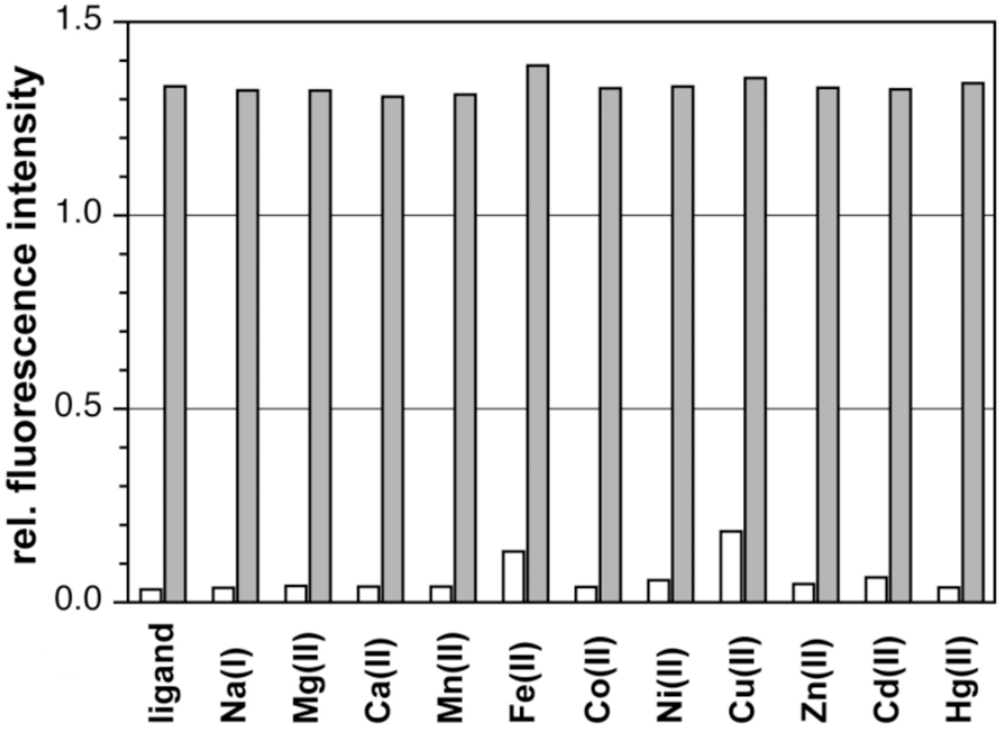

Fig. 3.

Fluorescence response of pyrazoline **1d** as a function of added metal cations in methanol (298 K, excitation at 345 nm, emission 436 nm). White bars: equimolar concentration of **1d** and the indicated metal cation. Grey bars: Competition with equimolar amount of [Cu(I)$(CH_3CN)_4]PF_6$ and the respective metal cation.

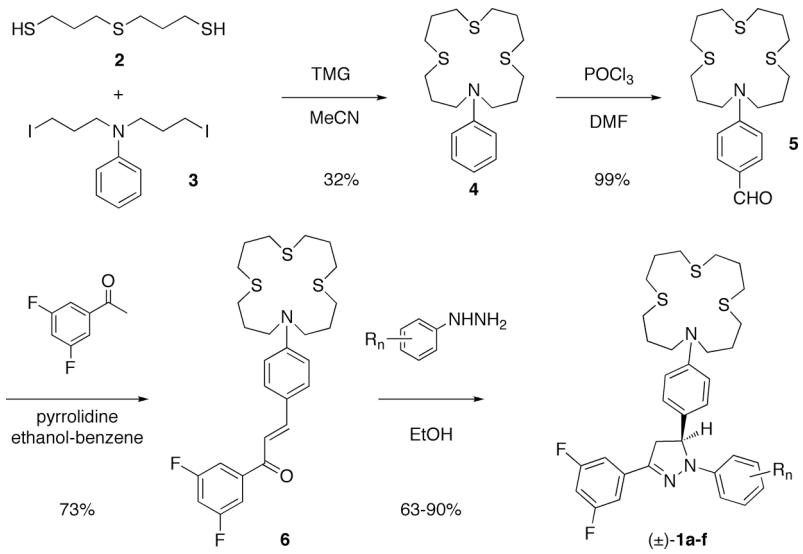

Scheme 1.
Synthesis of pyrazoline derivatives **1a-f** (a substituent key is provided in Table 1)

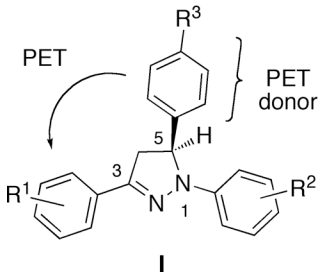

I

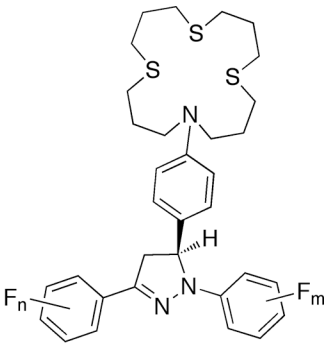

II

Chart 1.

Table 1

Photophysical Data of Pyrazoline Derivatives **1a-1f** in Methanol at 298K

compd	R	abs λ_{max}/nm	em λ_{max}/nm	Stokes shift/cm^{-1}	ΔE_{00}/cm^{-1}[a]	Φ_F[b]			f_e[c]	
						neutral[d]	acidic[e]	Cu(I)[f]	acidic	Cu(I)
1a	H	371	476	5950	23 980	0.058	0.23	0.20	4	3
1b	3-F	366	461	5630	24 510	0.029	0.36	0.19	12	7
1c	2,5-F_2	355	451	6000	25 170	0.0084	0.40	0.12	48	14
1d	2,3,5-F_3	350	436	5640	25 750	0.0014	0.47	0.07	335	50
1e	2,3,5,6-F_4	330	420	6440	27 060	n.d.[g]	0.21	0.024	-	-
1f	2,3,4,5,6-F_5	323	423	7320	27 300	n.d.[g]	0.044	0.0063	-	-

[a] Zero-zero transition energy; estimated based on $\Delta E_{00} = (E_{abs}(max)+E_{em}(max))/2$.

[b] fluorescence quantum yield; quinine sulfate as reference.

[c] fluorescence enhancement factor $f_e = \Phi_F/\Phi_{neutral}$.

[d] neat methanol.

[e] 180 mM trifluoroacetic acid in methanol.

[f] 10 μM $[Cu(I)(CH_3CN)_4]PF_6$ in methanol (0.1% acetonitrile).

[g] signal/noise ratio insufficient for accurate determination.

Table 2

Donor and acceptor reduction half-wave potentials and electron transfer parameters for pyrazoline derivatives **1a-f**.

compd	$E_{1/2}(D^+/D)/V^a$	$E_{1/2}(A/A^-)/V$	$\Delta E_{00}/eV^b$	$\Delta G_{et}/eV^c$
1a	0.46	−2.53	2.97	−0.03
1b	0.46	−2.50	3.04	−0.13
1c	0.48	−2.46	3.12	−0.23
1d	0.48	−2.42	3.19	−0.34
1e	0.49	−2.39	3.35	−0.52
1f	0.49	−2.35	3.38	−0.59

[a] Half-wave potential in acetonitrile/0.1 M Bu_4NPF_6 vs $Fc^{+/0}$ at 298K, glassy carbon working electrode, $Ag/AgNO_3$ reference electrode, 100 mV/s scan rate.

[b] Zero-zero transition energy in methanol; estimated based on $\Delta E_{00} = (E_{abs}(max)+E_{em}(max))/2$.

[c] Electron transfer free energy change calculated on the basis of the Rehm-Weller equation (1). The ion-pair stabilization energy was estimated to be $w_p = -0.045$ eV.[14]

Table 3

Predicted photoinduced electron transfer parameters of compounds **1a-f**.

compd	σ_2[a]	$E(A/A^-)/V$[b]	ΔE_{00}/eV[c]	$-\Delta E_{00}-E(A/A^-)$/eV
1a	0.03	−2.54	3.03	−0.49
1b	0.34	−2.50	3.13	−0.63
1c	0.59	−2.48	3.22	−0.74
1d	0.86	−2.45	3.31	−0.86
1e	1.07	−2.42	3.38	−0.96
1f	1.19	−2.41	3.42	−1.01
MUE[d]		0.024[d]	0.072[d]	0.056[d]

[a] Computational Hammett constant for the 1-aryl ring according to reference 16 (the 3-aryl ring is identical in all compounds with σ_2= 0.65).

[b] Acceptor potential calculated from LFER of eqn 2a.

[c] Zero-zero transition energy calculated from LFER of eqn 2b.

[d] Mean unsigned error.